Studies on formic acid-catalyzed dimerization of isorhapontigenin and of resveratrol to tetralins

ARTICLE *in* TETRAHEDRON · JUNE 2003

Impact Factor: 2.64 · DOI: 10.1016/S0040-4020(03)00623-9

Pergamon

SCIENCE DIRECT®

Tetrahedron 59 (2003) 4405–4413

TETRAHEDRON

Studies on formic acid-catalyzed dimerization of isorhapontigenin and of resveratrol to tetralins

Xiao-Mei Li, Kai-Sheng Huang, Mao Lin* and Li-Xin Zhou

Institute of Materia Medica, Chinese Academy of Medical Sciences and Peking Union Medical College, 1 Xian Nong Tan Street, Beijing 100050, People's Republic of China

Received 2 January 2003; revised 18 March 2003; accepted 10 April 2003

Abstract—The formic acid-catalyzed dimerization of stilbenes, isorhapontigenin and resveratrol, offers a route to tetralin derivatives. Seven products have been obtained, four of which were trisubstituted tetralins and three of which were formed from tetralins by losing substituted benzene groups and methoxy groups during the Diels–Alder reaction. The structures and configurational assignments of the compounds were elucidated mainly by spectroscopic analysis and a possible mechanism is proposed for the reaction. The anti-inflammatory activities of some derivatives obtained were also evaluated.

1. Introduction

Natural stilbene oligomers are a group of compounds mostly obtained from nine plant families, namely Dipterocarpaceae, Vitaceae, Cyperaceae, Leguminosae, Gnetaceae, Iridaceae, Celastraceae, Paeoniaceae and Moraceae.[1] Various biological activities, such as the activity of chemoprevention of cancer,[2] protein kinase C inhibition,[3] anti-HIV and cytotoxaty,[4] anti-fungal,[5] and cyclooxygenase (COX I, COX II) inhibition[2,6,7] have been found in recent years. During our studies on anti-inflammatory compounds from Gnetaceae and Vitaceae plants, more than 70 oligostilbenes were obtained.[1] In addition, a number of natural dimeric stilbenes exhibited potent anti-inflammatory activities, including inhibition of leukotriene (LTB_4, C_4, D_4) and its receptor antagonism, affinity of HL 60 and CEC multiplet in vitro and in vivo models.[7–11] Due to the scarcity of dimeric stilbenes in natural raw materials, further screening on anti-inflammatory compounds was difficult. In order to find leading compounds for drug development, a series of biomimetic syntheses were carried out.

The stilbene oligomers hitherto known fall into five (1–5) major groups, and each group is subdivided into A and B types.[1] Type A contains at least one five-membered oxygen heterocyclic ring, usually the *trans*-2-aryl-2,3-dihydrobenzofuran moiety. Type B does not contain any oxygen heterocyclic ring. Cyclodimeric stilbenes, indanes and tetralins are included in this type of oligostilbenes. Some derivatives of I-A, II-A groups with *trans*-2-aryl-2,3-dihydrobenzofuran moiety such as shegansu B and amurensin H had been prepared from natural isorhapontigenin and resveratrol, respectively, using iron (III) chloride[12,13] and silver oxide[14] as coupling agents. However, an acidic dimerization could afford different type of dimers. Kuo et al. reported that acidic dimerization of 3,4-dioxygenated cinnamate or 1-phenylpropene produced cyclomeric arylindane type products[15] and Aguirse et al. obtained indanes and tetralins by acid treatment of *trans*-stilbenes and N-1,2-diarylethylamide.[16,17] Similarly, for restrytisol C, a tetralin was obtained by the grapevine pathogen *Botrytis cinerea*.[6] In order to get various cyclooligostilbenes, we designed the dimerization method using natural isorhapontigenin and resveratrol as starting materials and referred to the above literature,[15] selecting 80% formic acid as a catalyst. A series of tetralins, isorhaformicols A (**2a**), B (**3a**), C (**4a**), D (**5a**) and resformicols A (**2b**), B (**3b**), C (**4b**) was obtained (Scheme 1). All structural assignments were made by various spectral evidence including 2D NMR techniques. Surprisingly, the structures of **4a** and **4b** were found to have lost a substituted phenyl group, 3-methoxy-*p*-hydroxyphenyl and *p*-hydroxy-phenyl, respectively, during dimerization. Moreover, **5a** successively lost two substituted benzene rings and one methoxy group during trimerization. These are reactions that have not been reported before.

The present work describes how, on the basis of spectroscopic data, it has been possible to perform the structural assignment, and to determine the stereochemistry of a series of cyclodimer tetralins with three stereogenic centers starting from isorhapontigenin or resveratrol. The probable mechanisms of cyclodimerization are discussed.

Keywords: tetralin; Diels–Alder reaction; formic acid; stilbenes; isorhapontigenin and resveratrol.

* Corresponding author. Tel.: +86-10-63165326; fax: +86-10-63017757; e-mail: linmao@imm.ac.cn

0040–4020/03/$ - see front matter
doi:10.1016/S0040-4020(03)00623-9

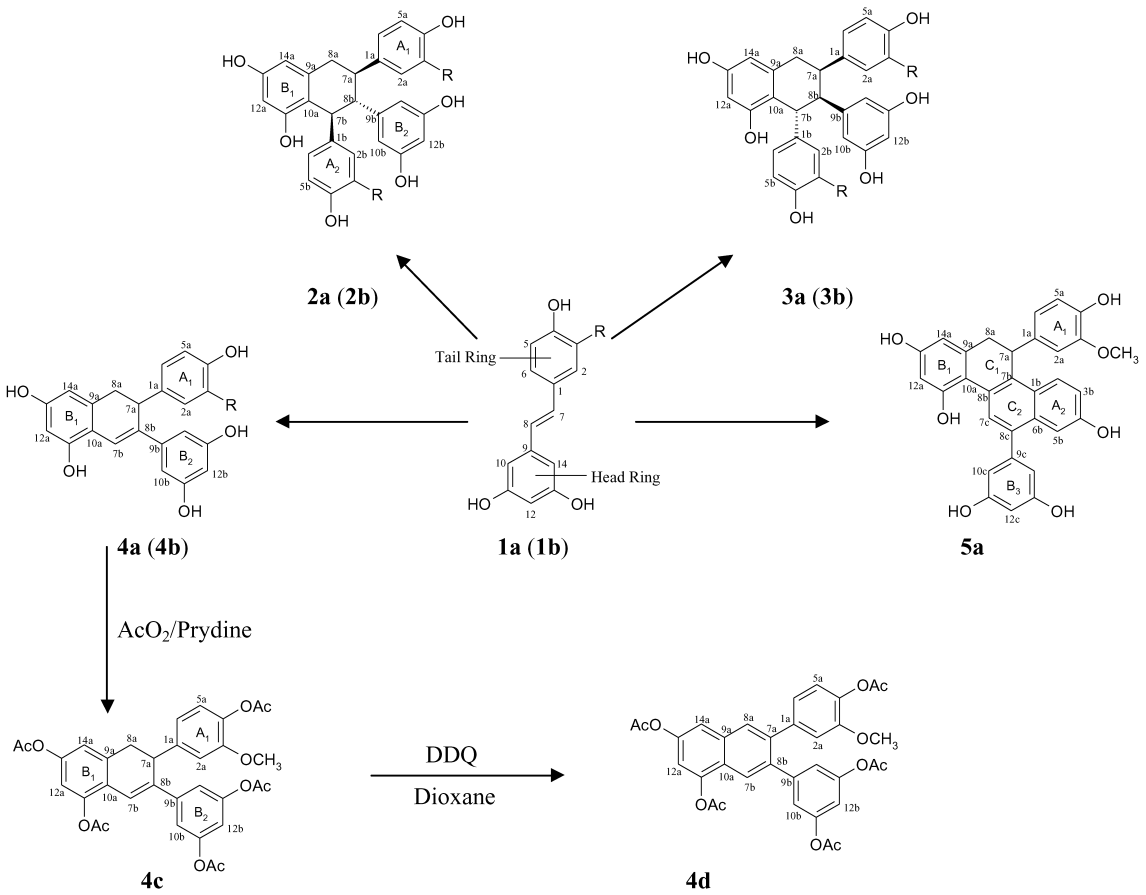

Scheme 1. Reaction products from isorhapontigenin (**1a**, R=OCH_3) and resveratrol (**1b**, R=H) with formic acid.

2. Results

The stilbene monomer isorhapontigenin (**1a**) and resveratrol (**1b**) were treated with formic acid respectively to yield seven compounds altogether. **2a**, **3a**, **4a**, **5a** were obtained from **1a**, and **2b**, **3b**, **4b** were produced from **1b** (see Table 1).

Isorhaformicol A (**2a**) and B (**3a**) were obtained as pale yellow amorphous powders with slightly visible darkened zone under UV light at 254 nm. The UV spectra showed λ_{max} 283 nm (**2a**) and λ_{max} 282 nm (**3a**). Both have the same molecular formula as $C_{30}H_{28}O_8$ at *m/z* 517 $[M+H]^+$ by LR-MS and HR-MS, which corresponds to a dimer of isorhapontigenin.

The mass spectrum of **2a** shows a base peak at *m/z* 393 for $[M^+-123$ ($C_7H_7O_2$, 3-methoxy-4-hydroxy-phenyl or 3,5-dihydroxy-benzyl)] and a prominent peak at *m/z* 259 of $[M/2+H]^+$ derived from a retro Diels–Alder type cleavage. The cleavage is characteristic of tetralins. The ^1H NMR spectrum of **2a** displayed two methoxy groups, two sets of ABX systems for rings A_1 and A_2, one AB_2 system for ring B_2, a pair of *meta*-coupled aromatic protons (see Table 2), two geminal signals appearing at δ 2.69 (dd, J_1=15.1 Hz, J_2=2.8 Hz, H-8a_1), 3.13 (dd, J_1=15.1 Hz, J_2=12.6 Hz, H-8a_2) and three aliphatic methine signals appearing at δ 3.01 (td, J_1=12.6 Hz, J_2=2.8 Hz, H-7a), 2.92 (dd, J_1=12.6 Hz, J_2=8.1 Hz, H-8b), 4.23 (d, J=8.1 Hz, H-7b), which were all correlated by ^1H–^1H COSY experiment. By

Table 1. Reaction products from isorhapontigenin or resveratrol

Starting material	Products	Yield (%)
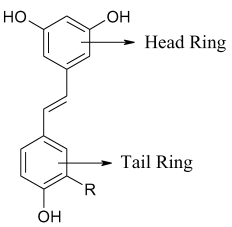	**2a**: R=OCH_3	8.91
	2b: R=H	20.00
	3a: R=OCH_3	4.46
	3b: R=H	3.20
1a: R=OCH_3	**4a**: R=OCH_3	48.72
	4b: R=H	12.60
1b: R=H	**5a**: R=OCH_3	1.48
	R=H	–

Table 2. ^{1}H and ^{13}C NMR data for compounds **2a**–**4a**

Position	**2a**[a]		**3a**[a]		**4a**[b]	
	^{1}H	^{13}C	^{1}H	^{13}C	^{1}H	^{13}C
1a		137.2		136.3		133.4
2a	6.67 (br s)	112.6	6.77 (d, 1.8)	113.2	6.72 (d, 1.8)	111.8
3a		148.3		148.0		147.2
4a		147.4		145.6		144.9
5a	6.56 (d, 8.4)	115.2	6.70 (d, 8.1)	115.1	6.51 (d, 8.1)	115.0
6a	6.55 (br s)	120.8	6.45 (dd, 8.1, 1.8)	121.5	6.43 (dd, 8.1, 1.8)	118.7
7a	3.01 (td, 12.6, 2.8)	48.0	3.32 (dt, 13.4, 4.5, 3.2)	38.7	3.82 (d, 6.6)	42.8
8a$_1$	2.69 (dd, 15.1, 2.8)	41.0	2.71 (dd, 16.6, 4.5)	32.3	2.70 (d, 16.2)	38.0
8a$_2$	3.13 (dd, 15.1, 12.6)		2.96 (dd, 16.6, 13.4)		3.15 (dd, 16.2, 6.6)	
9a		141.4		140.6		142.5
10a		118.1		116.7		113.4
11a		156.9		157.0		154.0
12a	6.19 (d, 2.2)	101.8	6.28 (d, 1.9)	101.6	5.88 (d, 1.5)	100.4
13a		157.1		157.3		157.4
14a	6.22 (d, 2.2)	106.8	6.28 (d, 1.9)	107.0	6.11 (d, 1.5)	106.9
1b		139.7		140.7		
2b	6.37 (d, 1.9)	113.3	6.19 (d, 1.8)	112.8		
3b		148.3		147.5		
4b		147.7		145.6		
5b	6.58 (d, 8.1)	115.2	6.58 (d, 8.1)	115.1		
6b	6.31 (dd, 8.1, 1.9)	120.4	6.22 (dd, 8.1, 1.8)	121.6		
7b	4.23 (d, 8.1)	50.3	4.42 (br s)	45.9	7.24 (s)	119.3
8b	2.92 (dd, 8.1, 12.6)	59.9	3.05 (d, 3.2)	56.2		134.0
9b		145.2		145.3		135.3
10 (14)b	5.95 (d, 2.1)	108.2	5.78 (d, 2.2)	108.7	6.31 (d, 2.1)	103.3
11 (13)b		158.6		158.4		158.2
12b	5.99 (t, 2.1)	100.8	6.14 (t, 2.2)	101.3	6.02 (t, 2.1)	101.0
3a-OCH$_3$	3.67 (s)	56.2	3.75 (s)	56.3	3.61 (s)	55.4
3b-OCH$_3$	3.57 (s)	56.1	3.55 (s)	56.1		55.4

[a] Measured in CD_3COCD_3 at 500 MHz for ^{1}H and 125 MHz for ^{13}C NMR respectively, with assignments confirmed by ^{1}H–^{1}H COSY, HMQC, HMBC and NOESY spectra.
[b] Measured in DMSO-d_6 at 300 MHz for ^{1}H and 75 MHz for ^{13}C NMR respectively, with assignments confirmed by ^{1}H–^{1}H COSY, HMQC, HMBC and NOESY spectra.

analysis of the HMQC spectrum, all the protonated carbons were assigned. The HMBC experiment aided the determination of the connectivities, especially the cross peaks between H-7a/C-2a, 6a; H-8a/C-10a, 14a; H-14a/C-8a; H-7b/C-9a, 11a, 2b, 6b, 9b; H-8b/C-8a, 1b, 10(14)b. According to the coupling constant of 15.1 Hz with the benzyl methylene group and the data of HMBC, the structure of **2a** was determined as a trisubstituted tetralin type.[16] The configuration of the three chiral centers in the cyclohexene ring could be determined by the key NOE interactions as H-7a/H-10(14)b, H-7b/H-10(14)b, H-8b/H-2a, 6a, 2b. From the above experiments, the relative configuration of H-7a, 8b, 7b in **2a** was determined to be in *trans*–*trans* orientation, namely the relative configuration of **2a** was *rel*-(7a*R*,7b*S*,8b*S*).

The EI-MS of **3a** showed the base peak at *m*/*z* 227 [M$^+$/2−31] and a prominent ion at *m*/*z* 393 [M$^+$−123]. The ^{1}H NMR spectrum of **3a** showed similar sets of aromatic proton resonances to **2a**. However, the splitting patterns of the aliphatic protons H-7a, H-8a, H-7b and H-8b differed considerably, while a striking similarity was noted with the chemical shifts in the ^{13}C NMR spectra of **3a** when compared with those of **2a**. It suggested that **3a** was a stereoisomer of **2a**. This conjecture was confirmed by analysis of the HMQC and HMBC experiments, especially by the cross peaks between H-2a/C-7a; H-6a/C-7a; H-7a/C-2a, 6a; H-8a/C-10a, 14a, 8b; H-14a/C-8a; H-6b/C-7b; H-7b/C-7a, 9a, 11a, 2b, 9b and H-8b/C-10a, 10(14)b, and the same connectivities of **3a** and **2a** were confirmed. The different coupling constant between aliphatic protons indicated a different orientation of the substituting benzene groups. NOE experiment supported the different orientation of H-7b, 8b, and 7a in the cyclohexene ring of **3a**. The significant correlations between H-7b/H-8a$_1$, H-7a/H-8b, H-8b/H-8a$_2$ were observed, which revealed that H-7a, 8b, 7b were in a *cis*–*trans* orientation. Therefore the relative configuration was determined to be *rel*-(7a*R*,7b*R*,8b*R*), as illustrated in **3a**.

Isorhaformicol C (**4a**) was obtained as a yellowish powder, exhibiting intense blue fluorescence under UV light at 254 nm. The UV spectrum with λ_{max} 290, 310 nm suggested the presence of an extended conjugation in the structure. The FABMS *m*/*z* 392 and HREIMS were in agreement with a molecular formula of $C_{23}H_{20}O_6$, not corresponding to a dimer. Acetylation of **4a** with acetic anhydride/pyridine at room temperature overnight gave colorless crystals of penta-acetylated derivative (**4c**) after recrystallization with MeOH. The significant fragment peaks in the EI-MS spectrum of **4c** at *m*/*z* 602, 560, 518, 476, 434 and 392 along with its ^{1}H NMR signals appearing at δ 2.24 (6H, 2×AcO), 2.26 (3H, 1×AcO), 2.28 (3H, 1×AcO), 2.37 (3H, 1×AcO) indicated the presence of five hydroxyl groups in the structure of **4a**, and it further confirmed the exact molecule weight of **4a** as 392. As the dimerization of two isorhapontigenin units would provide a *m*/*z* 516, it must have lost a 3-methoxy-4-hydroxy-phenyl ($C_7H_7O_2$)

Table 3. ^{1}H and ^{13}C NMR data for compounds **2b**–**4b**

Position	**2b**		**3b**		**4b**	
	^{1}H	^{13}C	^{1}H	^{13}C	^{1}H	^{13}C
1a		139.4		139.9		
2(6)a	6.72 (d, 8.4)	129.6	6.85 (d, 8.4)	129.8		
3(5)a	6.58 (d, 8.4)	115.5	6.47 (d, 8.4)	115.3[a]		
4a		155.8		155.9		
7a	4.26 (d, 6.9)	49.8	4.36 (s)	45.4	7.44 (s)	119.8
8a	2.97 (dd, 13.5, 6.9)	60.0	2.96 (d, 3.3)	56.4		135.7
9a		148.3		145.2		136.6
10(14)a	5.92 (d, 2.1)	108.0	5.66 (d, 2.1)	108.4	6.50 (d, 2.1)	104.4
11(13)a	6.00 (t, 2.1)	158.5	6.04 (t, 2.1)	158.2	6.18 (t, 2.1)	159.1
12a		101.0		101.2		101.9
1b		136.5		135.4		134.3
2(6)b	6.92 (d, 8.4)	129.2	6.45 (d, 8.7)	129.4	7.02 d (8.4)	129.3
3(5)b	6.58 (d, 8.4)	115.3	6.51 (d, 8.7)	115.2[a]	6.61 d (8.4)	115.8
4b		156.0		156.1		156.5
7b	3.04 (dd, 13.5,2.1)	47.9	3.23 (dt, 13.5, 4.2, 3.3)	37.3	3.94 dd (7.5, 1.5)	41.7
8b	2.69 (dd, 15.0, 2.1)	41.0	2.64 (dd, 16.5, 4.2)	31.4	2.79 (dd, 15.3, 1.5)	39.1
	3.15 (br d, 15.0)		2.89 (dd, 16.5, 13.5)		3.29 (dd, 15.3, 7.5)	
9b		141.4		140.6		144.2
10b		118.6		116.6		115.1
11b		156.7		156.7		154.9
12b	6.18 (d, 2.1)	101.9	6.22 s	101.5	6.25 d (2.1)	101.4
13b		157.0		157.0		158.4
14b	6.23 (d, 2.1)	106.8	6.22 s	107.1	6.04 d (2.1)	108.1

Measured in CD_3COCD_3 at 300 MHz for ^{1}H and 75 MHz for ^{13}C respectively, with assignments confirmed by ^{1}H–^{1}H COSY, HMQC, HMBC and NOESY spectra.

[a] May be interchanged within the same column.

fragment during dimerization. From the ^{1}H NMR spectrum of **4a**, one methoxy group, one set of ABX system for ring A_1, one set of AB_2 system for ring B_2, two *meta*-coupled protons for ring B_1 and a single olefinic proton were observed together with the coupled aliphatic methine and methylene signals. The ^{13}C NMR spectrum of **4a** was missing six aromatic carbons and a methoxyl carbon compared with isorhapontigenin dimers and it was also missing two aliphatic methine protons and one set of ABX system and more than two quaternary carbons, in contrast to **2a** and **3a**. On the basis of ^{1}H–^{1}H COSY, HMQC, and especially the key cross peaks between H-7a/C-6a, 9a, 7b, 9b; H-8a/C-10a, 14a; H-14a/C-8a; H-7b/C-7a, 9a, 11a, 9b; H-8b/C-8a, 10(14)b and H-10(14)b/C-8b in HMBC experiment, the structure was determined to be **4a**, as illustrated in Scheme 1. NOE interactions between H-2a/H-10(14)b, H-7a/H-2a, H-7a/H-10(14)b, H-7b/H-10(14)b further confirmed the structure. The structure of **4a** was further verified by dehydrogenation of **4c** with 2,3-dichloro-5,6-dicyano-1,4-benzoquinone (DDQ) in dry dioxane to afford the aromatised compound **4d**.

The corresponding des-methoxy compounds (R=H) **2b**–**4b** were obtained from **1b** as starting material. The relative structures were determined by spectroscopic analysis, and the ^{1}H and ^{13}C NMR data are shown in Table 3.

Isorhaformicol D (**5a**) was obtained as black amorphous powder, showing intense blue fluorescence under UV light 254 nm. The UV spectrum with λ_{max} 288, 348 nm revealed

Table 4. ^{1}H and ^{13}C NMR data for compound **5a**

Position	^{1}H	^{13}C	Position	^{1}H	^{13}C
1a		134.9	1b		132.1
2a	6.74 (d, 1.5)	111.8	2b	7.95 (d, 8.9)	124.4
3a		147.2	3b	7.59 (dd, 8.9, 1.8)	125.3
4a		144.9	4b		151.5
5a	6.52 (d, 8.1)	114.6	5b	8.41 (d, 1.8)	120.0
6a	6.48 (dd, 8.1, 1.5)	120.6	6b		124.2
7a	4.77 (d, 5.2)	38.8	7b		125.4
8a	2.98 (dd, 14.9, 1.3)	39.0	8b		132.6
	3.25 (dd, 14.9, 5.2)				
9a		138.9	7c	8.21 (s)	109.9
10a		114.7	8c		136.1
11a		155.8	9c		143.5
12a	6.35 (d, 1.5)	102.3	10(14)c	6.72 (d, 2.1)	105.7
13a		157.6	11(13)c		159.2
14a	6.14 (d, 1.5)	108.5	12c	6.33 (t, 2.1)	101.8
3a-OCH_3	3.57 (s)	55.3			

Measured in CD_3COCD_3 at 500 MHz for ^{1}H and 75 MHz for ^{13}C NMR respectively, with assignments confirmed by ^{1}H–^{1}H COSY, HMQC, HMBC and NOESY spectra.

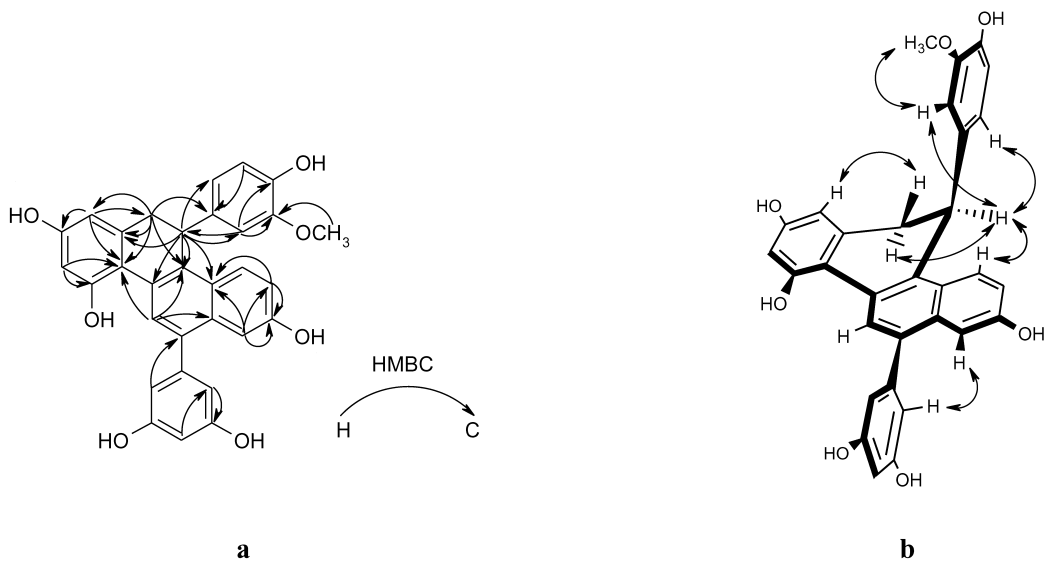

Figure 1. Significant long-range CH correlations in the HMBC spectrum (a) and NOE interactions in the NOESY spectrum (b) of **5a**.

the presence of a conjugated system in the structure. From FABMS *m/z* 509 $[M+1]^+$, together with the ^{13}C NMR, the molecular formula was determined as $C_{31}H_{24}O_7$ with 20 degrees of unsaturation, which was further confirmed by its HRESIMS. The ^1H NMR spectrum of **5a** (Table 4) displayed two sets of ABX systems for ring A_1 and A_2, one AB_2 system for ring B_3, a pair of *meta*-coupled aromatic protons for ring B_1, a single aromatic proton, one methoxy group, two geminal aliphatic protons and a methine proton. Only one methoxy group was observed in the spectrum indicating the methoxy group may be located on ring A_1 or ring A_2. The ^{13}C NMR and DEPT spectra of **5a** showed 31 carbons altogether, including one secondary aliphatic carbon, one methoxy group carbon, 12 aromatic tertiary carbons, one aliphatic tertiary carbon and 16 quaternary carbons. The chemical shifts of the geminal methylene protons and their coupling constant (J=14.9 Hz) suggested that it was a tetralin derivative. Thus the structure of **5a** should include five aromatic rings and one aliphatic ring (C_1) in the structure according to the above information. The single aromatic proton at δ 8.21 might be located on one substituted benzene ring (C_2).The downfield chemical shift values of the aromatic single proton at δ 8.21 and one ABX system for ring A_2 appearing at δ 7.95, 7.59 and 8.41 indicated an unusual chemical environment. H-7c may form a hydrogen bond with 11a hydroxyl and shift downfield. In the FABMS spectrum of **5a**, the prominent ion *m/z* 385 $[M-124]^+$ corresponded to $[M-C_7H_7O_2]^+$, which suggested the existence of 3-methoxy-*p*-hydroxy-phenyl fragment in the structure of **5a**.

The connectivities of **5a** for each ring were determined by HMBC cross peaks (Fig. 1a). NOE interactions (Fig. 1b) also confirmed the connective correlation. Thus, the structure was elucidated as shown in **5a**, it has a benzodihydrophenanthrene skeleton portion, which can

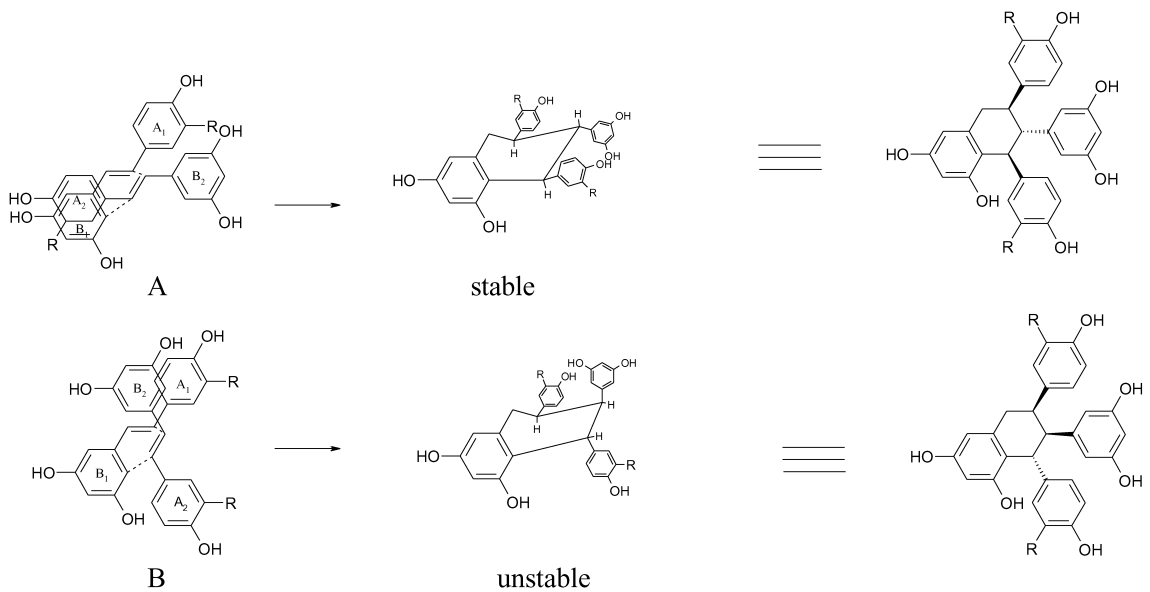

Scheme 2. Possible transition state in **1a** and **1b** dimerization process.

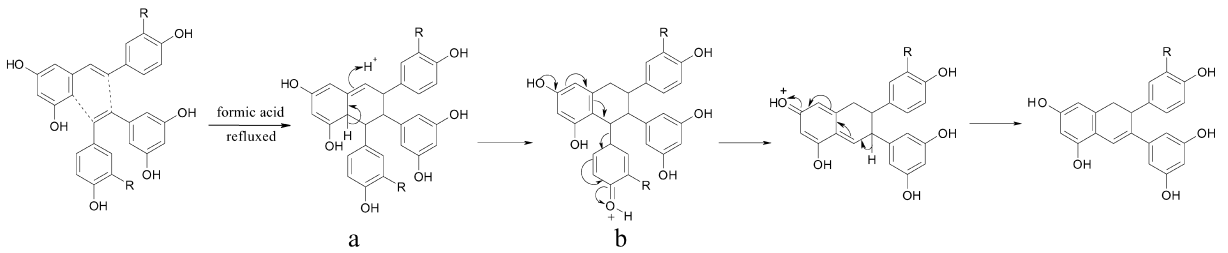

Scheme 3. Proposed mechanism of **1a** and **1b** dimerization losing the aryl ring.

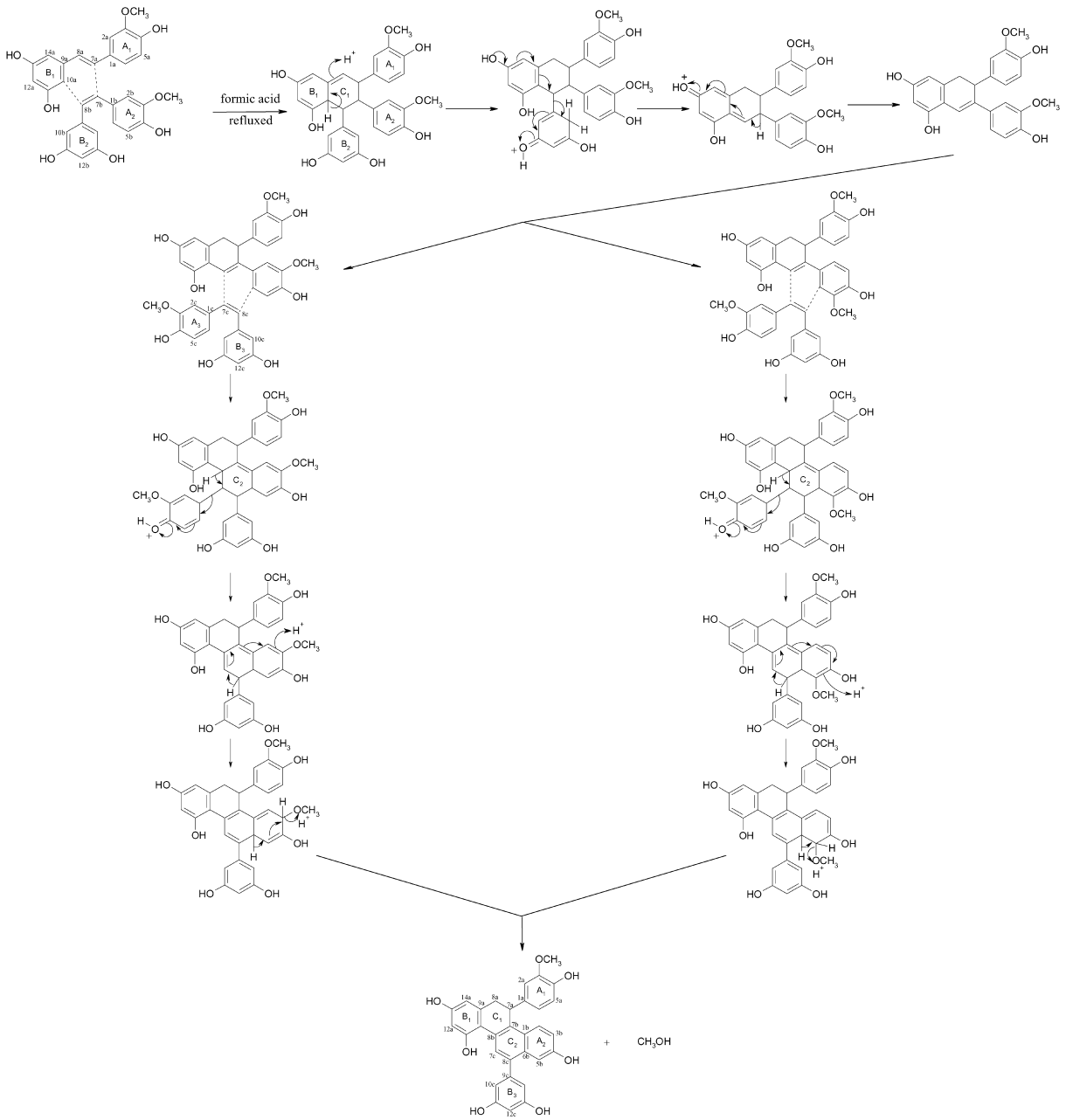

5a

Scheme 4. Proposed mechanism of 1a trimerization to **5a**.

explain the special chemical shift values of H-2b, 3b, 5b and 7c. The possible mechanism will be discussed later on.

3. Discussion

The Diels–Alder reaction is a [4+2] cycloaddition of a diene and a dieneophile to form a six-membered ring. The stilbene monomers **1a** and **1b** contain extended conjugate systems which can react as both diene and dienophile moieties. All the seven synthetic products can be resolved as two types of Diels–Alder adducts.

(1) Normal [4+2] adducts forming the benzo-cyclohexene system. The all *trans* adducts with the six-membered benzo-cyclohexene system are the major products as compared with the *cis*–*trans* (H-7a, 8b, 7b) adducts probably for the following reasons:

(a) The process of cyclodimerization to a trisubstituted tetralin is carried out starting from a dimeric carbocation.[15] A dimeric carbocation could be formed from two molecules of *trans*-stilbene by acid treatment. In the studied cases, the substrates **1a** and **1b** have 3-methoxy-4-hydroxy-phenyl, *p*-hydroxy-phenyl respectively and 3,5-dihydroxy-phenyl type substitution, leading to the carbocation in the 7a or 7b position of the starting materials.

(b) The coupling of phenoxyl radicals occurs fastest at the position of highest free electron densities except where there is steric hindrance to their approach. When the two functional groups approach as shown in Scheme 2A, the two aromatic rings A_2 and B_1 are in a parallel state, the electric cloud of the two aromatic rings overlapping to the greatest extent. This transition state is favorable to the process of the Diels–Alder reaction from the viewpoint of molecular orbital theory. Due to all three substituted benzene groups being in the equatorial orientation in the cyclohexene ring in Scheme 2A, the configuration of this structure was relatively stable. On the other hand, in Scheme 2B, two aromatic rings were in the axial orientation, causing a large spacial congestion; therefore this configuration was disfavored. Therefore the coupling reaction gave the all *trans* adducts as the major product and the *cis*–*trans* adducts were less favored due to the steric hindrance.

(2) Adducts losing substituted benzene ring or other substituents.

Compounds **4a**,**4b** and **5a** were adducts formed by loss of substituted benzene rings. Two molecules of **1a** or **1b** coupled by a head–tail connection, respectively. In the transition state structure, a and b were unstable (Scheme 3), losing a substituted benzene ring to produce the more stable structure of **4a** or **4b** with an extended conjugated system.

The formation of product **5a** would be possibly explained by reaction of three molecules of **1a** (Scheme 4). The first procedure produced a head–head and tail–tail connected dimer. The second step lost an aromatic ring (B_2), and then the product coupled with the third molecule of **1a**, after the cyclo-addition reaction and lost another substituted aromatic ring (A_3) and a methoxy group, finally forming **5a**. It is a special reaction, losing aryl rings and methoxy group during Diels–Alder reaction.

With **1b** as a starting material, no compound like **5a** was obtained, perhaps no such adducts were produced due to the absence of the methoxy group on the 4-hydroxy-phenyl ring.

4. Conclusion

It may be concluded that in the studied cases, the strong electron-donor substituents lead to a 6-atom ring. In our investigation of the Diels–Alder reaction from **1a** and **1b**, we found a side reaction involving loss of a substituted benzene ring during dimerization or trimerization, driven by ejection of methoxy group. It is a very special reaction we have not ever seen before. It may be formed through some transition states as shown in Schemes 3 and 4.

Table 5. Mass spectral data of the obtained tetralin derivatives

No.	M^+	$M^+/2$	M^+-Bz	M^+-Ar		Other
2a	517 (98)[a]	259 (30)	393 (100, or M^+-Ar)			Bz: 3,5-$(OH)_2C_6H_3CH_2$ Ar: 3-(CH_3O)-4-OH–C_6H_3
3a	516 (36)	258 (68) ↓−31 227 (100)[b]	393 (86, or M^+-Ar)			
4a	392 (100)	–	255 (9)	283 (12) 269 (41)	137 (Bz, 18)	Bz: 3-(CH_3O)-4-OH–$C_6H_3CH_2$ Ar: 3,5-$(OH)_2C_6H_3$, 3-(CH_3O)-4-OH–C_6H_3
2b	456 (48)	227 (100) ↓−16 211 (78)	349 (13) 333 (30)	362 (17)		Bz: 4-OH–$C_6H_3CH_2$ 3,5-$(OH)_2C_6H_3CH_2$ Ar: 4-OH–C_6H_4
3b	456 (78)	227 (100)[b] ↓−16 211 (77)	349 (45) 333 (60)	362 (32)		
4b	362 (100)	–	255 (24) ↓−16 239 (58)			Bz: 4-OH–$C_6H_4CH_2$

[a] The peak at *m*/*z* 517 (M^++H) was provided by FAB-MS.
[b] The fragment at *m*/*z* 227 was ($M^+/2-1$).

After comparison of mass spectra of the obtained tetralin derivatives (see Table 5), we draw the following conclusions.

The base peak mainly originates from a retro Diels–Alder type cleavage, and it gave $M^+/2$ as base peak in our studied cases. If there is an electron donor substituent on the aromatic ring, the content of M^+-Ar fragment will increase. In **4a** and **4b**, the base peaks were M^+ for their more stable structure with long conjugated system.

The anti-inflammatory activities have been tested. The inhibitory rates on LTB_4 biosynthesis for **2a**, **3a**, **4a** and **4d** at concentrations of 10^{-5} mol L^{-1} were 46, 51, 28 and 35%, respectively. The inhibitory rates on adhesion ability of HL-60 cell and CEC for **2b**, **3b** and **4b** at concentrations of 10^{-5} mol L^{-1} were 75.4, 60.2 and 66.3%, respectively. The inhibitory rates of leukotriene D_4 (LTD_4) receptor antagonism for **2b**, **3b**, **4b** at concentrations of 10^{-5} mol L^{-1} were 26, 40 and −15.7%, respectively. **2a**, **3a**, **2b** and **3b** showed potent anti-inflammatory activities.

5. Experimental

5.1. Plant material

The starting material **1a** was obtained directly from the lianas of *Gnetum montanum* Markgr. *f. megalocarpum* Markgr., which were collected at Dadugang in Jinghong country of Yunnan Province, People's Republic of China, in July 1999, and **1b** was obtained from the lianas of *Gnetum parvifolium* (Warb.) C. Y. Cheng, which were collected from Guangxi province of China in the spring. Both of the two species of Gnetaceae plants were identified by Professor W.- Z. Song, Institute of Materia Medica, Chinese Academy of Medical Sciences and Peking Union Medical College. The two voucher specimens have been deposited in the herbarium of this institute.

5.2. General

Melting points were determined on a XT_4-100X micro-melting point apparatus and were uncorrected. UV spectra were taken on a Shimadzu UV-260 spectrophotometer. IR spectra were run on a Nicolet Impact 400 infrared spectrometer recorded as KBr pellets. The NMR spectra were carried out on a Bruker AM-500 or a Varian Mercury-300 spectrometer using TMS as internal standard. EIMS and FABMS were taken on an Autospec-Ulma-Tof mass spectrometer, HRESIMS were obtained using a Bruker Daltonics Inc., APEX II mass spectrometer. HPLC was performed on a Waters 510 instrument equipped with an UV detector. TLC was conducted on silica gel GF_{254} (Qing Dao Hai Yang Chemical Group Co.).

5.3. General experimental procedures for cyclization in formic acid

5.3.1. General procedures for cyclomers 2a, 3a, 4a, and 5a obtained from 1a. A solution of **1a** (2.58 g, 0.01 mol) was refluxed in 15 mL 80% formic acid (0.29 mol) for 2.5 h. The reaction solution was neutralized with 10% aqueous NaOH, then extracted with ethyl acetate. The EtOAc extract was dried with anhydrous sodium sulfate for 24 h and evaporated to dryness in vacuo. Then the extract was subjected to repeated column chromatography ($CHCl_3$–MeOH–H_2O of 8:2.5:1) and preparative HPLC with a variety of solvent systems (MeOH–H_2O of 2:3, 3:4, 155:145), yielding **2a** (230 mg), **3a** (115 mg), **4a** (955 mg), **5a** (25 mg), respectively.

5.3.2. General procedures for cyclomers 2b, 3b, and 4b obtained from 1b. With similar procedure to those of **1a**, **1b** (1 g) was refluxed for 2 h in formic acid (30 mL) to yield **2b** (200 mg), **3b** (32 mg) and **4b** (100 mg).

5.3.3. Isorhaformicol A (2a). Yellow amorphous powder; mp 171–172°C; UV (EtOH) λ_{max} (log ε): 283 (4.09) nm; IR (KBr) ν_{max}: 3359, 1603, 1514, 1452, 1273, 1146, 1030, 839 cm^{-1}; ^1H (CD_3COCD_3, 500 MHz) and ^{13}C (CD_3-$COCD_3$, 125 MHz) NMR data see Table 2; FAB-MS *m/z* 517 $[M^++H]$ (98), 393 (M^+-123) (100), 259 ($M^+/2$) (30); HR-ESIMS calcd for $C_{30}H_{29}O_8$, *m/z* 517.1857 $[M+H]^+$, found 517.1844 (the relative error is 2.5 ppm).

5.3.4. Isorhaformicol B (3a). Yellow amorphous powder; mp 184–185°C; UV (EtOH) λ_{max} (log ε): 282 (3.89) nm; IR (KBr) ν_{max}: 3369, 1601, 1514, 1454, 1273, 1146, 1034, 843 cm^{-1}; ^1H (CD_3COCD_3, 500 MHz) and ^{13}C (CD_3-$COCD_3$, 125 MHz) NMR data see Table 2; EI-MS *m/z* 516 $[M]^+$ (36), 393 (M^+-123) (86), 258 ($M^+/2$) (68), 227 ($M^+/2-31$) (100); HR-EIMS calcd for $C_{30}H_{28}O_8$, *m/z* 516.1784 $[M]^+$, found 516.1755 (the relative error is 5.7 ppm).

5.3.5. Isorhaformicol B (4a). Yellow amorphous powder; mp 179–180°C; UV (EtOH) λ_{max} (log ε): 290 (4.06), 310 (4.07) nm; IR (KBr) ν_{max}: 3321, 2935, 1614, 1587, 1512, 1464, 1429, 1346, 1275, 1257, 1149, 1126, 1032, 839 cm^{-1}; ^1H (DMSO-d_6, 300 MHz) and ^{13}C (DMSO-d_6, 75 MHz) NMR data see Table 2; FAB-MS *m/z* 392 $[M]^+$ (100), 283 (M^+-109) (12), 269 (M^+-123), (41), 255 ($M^+-123-14$), (9), 137 (123+14) (18); HR-EIMS calcd for $C_{23}H_{18}O_6$, *m/z* 392.1260 $[M]^+$, found 392.1292 (the relative error is 8.2 ppm).

5.3.6. Penta-acetylated isorhaformicol B (4c). A solution of **4a** (200 mg) in Ac_2O (3 mL) and pyridine (3 mL) was left for 48 h at room temperature. White precipitate (448 mg) was obtained after adding water into the reaction mixture. The precipitate was recrystallized with MeOH to provide colorless crystals **4c** (150 mg); mp 102–103°C; EI-MS *m/z*: 602 $[M]^+$, 560, 518, 476, 434, 392. ^1H ($CDCl_3$, 500 MHz) data: δ 6.67 (1H, br s, H-2a), 6.89 (1H, d, *J*=8.1 Hz, H-5a), 6.77 (1H, dd, *J*=8.1, 2.1 Hz, H-6a), 3.99 (1H, d, *J*=7.5 Hz, H-7a), 2.95 (1H, d, *J*=14.2 Hz, H-8a_1), 3.48 (1H, dd, *J*=14.2, 7.5 Hz, H-8a_2), 6.99 (1H, br s, H-12a), 6.68 (1H, br s, H-14a), 7.00 (1H, s, H-7b), 6.98 (2H, d, *J*=2.1 Hz, H-10(14)b), 6.83 (1H, t, *J*=2.1 Hz, H-12b), 3.61 (3H, s, OCH_3), 2.24 (6H, s, 2×OAc), 2.26 (3H, s, 1×OAc), 2.28 (3H, s, 1×OAc), 2.37 (3H, s, 1×OAc).

5.3.7. Dehydrogenated penta-acetylated isorhaformicol B by DDQ (4d). Compound **4c** (92 mg) was dissolved in 15 mL dried dioxane, then 120 mg DDQ in 15 mL dried

dioxane was added, and the reaction mixture was stirred under reflux for 40 h. The mixed solution was evaporated to dryness, which was purified by silica gel column chromatography ($CHCl_3$–MeOH, 200:1) and then recrystallized with $CHCl_3$–MeOH to give colorless crystals **4d** (70 mg); mp 144–145°C; EI-MS *m/z*: 600 $[M]^+$, 558, 516, 474, 432, 390. ^1H ($CDCl_3$, 300 MHz) data: δ 6.61 (1H, d, J=2.1 Hz, H-2a), 7.02 (1H, d, J=8.1 Hz, H-5a), 6.92 (1H, dd, J=8.1, 2.1 Hz, H-6a), 7.90 (1H, s, H-8a), 7.17 (1H, d, J=2.1 Hz, H-12a), 7.54 (1H, d, J=2.1 Hz, H-14a), 7.87 (1H, s, H-7b), 6.81 (2H, d, J=2.1 Hz, H-10(14)b), 6.82 (1H, t, J=2.1 Hz, H-12b), 3.59 (3H, s, OCH_3), 2.25 (6H, s, 2×OAc), 2.31 (3H, s, 1×OAc), 2.36 (3H, s, 1×OAc), 2.47 (3H, s, 1×OAc). In the NOESY spectrum the correlations between H-2a/OCH_3, H-8a/H-6a, H-8a/H-14a, H-10(14)b/H-7b, H-10(14)b/H-2a were observed.

5.3.8. Isorhaformicol D (5a). Black amorphous powder; mp 233–234°C; UV (MeOH) λ_{max} (log ε): 288 (4.60), 348 (4.11) nm; IR (KBr) ν_{max}: 3311, 1599, 1512, 1456, 1385, 1319, 1271, 1207, 1155, 1140, 1022, 1003, 818 cm^{-1}; ^1H (CD_3COCD_3, 500 MHz) and ^{13}C (CD_3COCD_3, 75 MHz) NMR data see Table 4; FAB-MS *m/z* 509 $[M+H]^+$; HR-ESIMS calcd for $C_{31}H_{25}O_7$, *m/z* 509.1595 $[M+H]^+$, found 509.1581 (the relative error is 2.7 ppm), calcd for $C_{24}H_{17}O_5$, *m/z* 385.1076 $[M-C_7H_7O_2]^+$, found 385.1113 (the relative error is 9.6 ppm).

5.3.9. Resformicol A (2b). Colorless amorphous powder; mp 202–203°C; UV (MeOH) λ_{max} (log ε): 280 (3.68) nm; IR (KBr) ν_{max}: 3305, 2902, 1614, 1599, 1512, 1452, 1325, 1232, 1142, 1047, 999, 831 cm^{-1}; ^1H NMR (CD_3COCD_3, 300 MHz) and ^{13}C NMR (CD_3COCD_3, 75 MHz) data, see Table 3; EIMS *m/z* 456 $[M]^+$ (48), 362 (M^+-94) (17), 349 ($M^+-94-13$) (13), 333 (M^+-123) (30), 227 ($M^+/2-1$) (100), 211 ($M^+/2-16$) (78); HR-EIMS calcd for $C_{28}H_{24}O_6$, *m/z* 456.1573 $[M]^+$, found 456.1594 (the relative error is 4.5 ppm).

5.3.10. Resformicol B (3b). Colorless amorphous powder; mp 214–215°C; UV (MeOH) λ_{max} (log ε): 280 (3.78) nm; IR (KBr) ν_{max}: 3367, 2904, 1612, 1597, 1512, 1448, 1348, 1227, 1142, 1034, 984, 839 cm^{-1}; ^1H NMR (CD_3COCD_3, 300 MHz) and ^{13}C NMR (CD_3COCD_3, 75 MHz) data, see Table 3; EIMS *m/z* 456 $[M]^+$ (78), 362 (M^+-94) (32), 349 ($M^+-94-13$) (45), 333 (M^+-123) (60), 227 ($M^+/2-1$) (100), 211 ($M^+/2-16$) (77); HR-EIMS calcd for $C_{28}H_{24}O_6$, *m/z* 456.1573 $[M]^+$, found 456.1545 (the relative error is 6.1 ppm).

5.3.11. Resformicol C (4b). Yellowish amorphous powder; mp 152–153°C; UV (MeOH) λ_{max} (log ε): 289 (sh), 311 (4.07), 334 (4.16) nm; IR (KBr) ν_{max}: 3305, 2931, 1684, 1612, 1510, 1456, 1346, 1250, 1147, 1034, 1001, 982, 835 cm^{-1}; ^1H NMR CD_3COCD_3, 300 MHz) and ^{13}C NMR (CD_3COCD_3, 75 MHz) data, see Table 3; EIMS *m/z* 362 $[M]^+$ (100), 255 (M^+-107) (24), 239 ($M^+-107-16$) (58); HR-EIMS calcd for $C_{22}H_{18}O_5$, *m/z* 362.1154 $[M]^+$, found 362.1131 (the relative error is 6.5 ppm).

Acknowledgements

This research program was supported by the National Natural Science Foundation of China (No. 30070889). The authors are grateful to Professor X. T. Liang of our institute, for advice on deduction of special reaction and thank Professor G. F. Cheng for the pharmacological test. The authors thank the Department of Instrumental Analysis of our institute, for the measurement of UV, IR, NMR and MS spectra, and thank Beijing Mass Spectrometry Center, Institute of Chemistry, Chinese Academy of Sciences, for measurement of HR-ESIMS spectra.

References

1. Li, N.; Li, X. M.; Huang, K. S.; Lin, M. *Acta Pharm. Sin.* **2001**, *36*, 944–950.
2. Jang, M.; Cai, L.; Udeani, G. O.; Slowing, K. V.; Thomas, C. F.; Beecher, C. W. W.; Fong, H. H. S.; Farnsworth, N. R.; Kinghorn, A. D.; Mehta, R. G.; Moon, R. C.; Pezzuto, J. M. *Science* **1997**, *275*, 218–220.
3. Kulanthaivel, P.; Janzen, W. P.; Ballas, L. M.; Jiang, J. B.; Hu, C. Q.; Darges, J. W.; Seldin, J. C.; Cofield, D. J.; Adamas, L. M. *Planta Med.* **1995**, *61*, 41–44.
4. Dai, J. R.; Hallock, Y. F.; Cadellina, J. H., II; Boyd, M. R. *J. Nat. Prod.* **1998**, *61*, 351–353.
5. Ducrot, P. H.; Kollmann, A.; Bala, A. E.; Majira, A.; Kerhoas, L.; Delorme, R.; Einhorn, J. *Tetrahedron Lett.* **1998**, *39*, 9655–9658.
6. Cichewicz, R. H.; Kouzi, S. A.; Hamann, M. T. *J. Nat. Prod.* **2000**, *63*, 29–33.
7. Chen, J. Master Thesis, Chinese Academy of Medical Sciences and Perking Union Medical College, 1997.
8. Zhao, N.; Zhu, X. Y.; Cheng, G. F. *Acta Pharm. Sin.* **1996**, *31*, 875–877.
9. Li, Y. T.; Zhong, M.; Deng, Y. J.; Zhu, X. Y.; Cheng, G. F. *Acta Pharm. Sin.* **1999**, *34*, 189–191.
10. Hu, Y. N.; Zhu, X. Y.; Liang, X. L.; Cheng, G. F. *Acta Pharm. Sin.* **2001**, *36*, 81–83.
11. Qi, H.; Cheng, G. F.; Zhang, C. Y.; Li, L. C. *Acta Pharm. Sin.* **2000**, *35*, 173–176.
12. Zhou, L. X.; Lin, M. *Acta Pharm. Sin.* **2000**, *35*, 669–674.
13. Huang, K. S.; Lin, M.; Wang, Y. H. *Chin. Chem. Lett.* **1999**, *10*, 817–820.
14. Zhou, L. X.; Lin, M. *Chin. Chem. Lett.* **2000**, *11*, 515–516.
15. Kuo, Y. H.; Wu, C. H.; Wu, R. E.; Lin, S. T. *Chem. Pharm. Bull.* **1995**, *43*, 1267–1271.
16. Aguirre, J. M.; Alesso, E. N.; Iglesias, G. Y. M. *J. Chem. Soc., Perkin Trans. 1* **1999**, 1353–1358.
17. Botta, B.; Iacomacci, P.; Vinciguerra, V.; Monache, G. D.; Gacs-Baitz, E.; Botta, M.; Misiti, D. *Chem. Pharm. Bull.* **1990**, *38*, 3238–3241.